

Shear behaviour of RC T-beams strengthened with U-wrapped GFRP sheet

K.C.Panda*¹, S. K. Bhattacharyya², and S. V. Barai³

¹Department of Civil Engineering, ITER, SOA University, 756113, India

²CSIR-Central Building Research Institute, Roorkee, 247667, India

³Department of Civil Engineering, IIT Kharagpur, 721302, India

(Received August 25, 2010. Revised June 28, 2011, Accepted November 25, 2011)

Abstract. This paper presents an experimental investigation on the performance of 2.5 m long reinforced concrete (RC) T-beams strengthened in shear using epoxy bonded glass fibre fabric. Eighteen (18) full scale, simply supported RC T-beams are tested. Nine beams are used as control beam specimens with three different stirrups spacing without glass fibre reinforced polymer (GFRP) sheet and rest nine beams are strengthened in shear with one, two, and three layers of GFRP sheet in the form of U-jacket around the web of T-beams for each type of stirrup spacing. The objective of this study is to evaluate the effectiveness, the cracking pattern and modes of failure of the GFRP strengthened RC T-beams. The test result indicates that for RC T-beams strengthened in shear with U-jacketed GFRP sheets, increase the load carrying capacity by 10-46%.

Keywords: reinforced concrete (RC); strengthening; glass fibre reinforced polymer (GFRP); shear strength; T-beams

1. Introduction

Civil engineering structures such as bridges, monumental buildings, tall towers, dams, harbours, offshore structures etc. deteriorate due to several reasons. The deterioration of the structures is primarily due to ageing, aggressive environment, industrial pollution, faulty design or construction and different natural disasters. Rebuilding of the deteriorating infrastructure is a major problem, faced by the nation today due to economical crisis and availability of funds. Therefore, the development of new rehabilitation and strengthening techniques which are safe, efficient and cost effective presents a formidable challenge for the construction industry. The use of externally applied fibre reinforced polymer (FRP) as a strengthening element for reinforced concrete structures is gaining tremendous popularity and interest because of its high strength to weight ratio, high stiffness to weight ratio, corrosion resistance, durability, non magnetic, non conductive, high resistance to chemical attack as well as the ease in installation.

Most of the research studies and field applications, however, were undertaken for flexural strengthening and for retrofitting of columns. Research studies on shear strengthening with fibre reinforced polymer are sparse and are mostly limited to relatively small beams and the research in this area exist since 1992

* Corresponding author, Ph.D., E-mail: kishoriit@gmail.com

(Berset 1992). Shear failure of an RC beam is a type of failure mode that has a catastrophic effect. If an RC beam, deficient in shear strength, is over loaded, shear failure may occur suddenly without advance warning of distress. Shear deficiency of the beam may occur due to many reasons such as insufficient shear reinforcement or reduction in steel area due to corrosion, increased service load and construction errors. In addition, there is an urgent need to upgrade the shear resistance of older RC structures to meet the current seismic design standards in high seismic regions. In this situation externally bonded FRP reinforcement may be used efficiently in strengthening the concrete beams, weak in shear.

A number of important contributions involving the analytical studies of RC beams with externally bonded FRP in shear are present in the literature (e.g. Chaallal *et al.* 1998, Triantafillou 1998, Triantafillou and Antonopoulos 2000, Khalifa *et al.* 1998, Chen and Teng 2003a, 2003b). The experimental studies on RC rectangular beams, strengthened with FRP in shear have been carried out by several researchers (Al-Sulaimani *et al.* 1994, Noris *et al.* 1997, Li *et al.* 2001, Khalifa and Nanni 2002, Pellegrino and Modena 2002, Taljsten 2003, Zhang and Hsu 2005, Adhikary *et al.* 2004, Cao *et al.* 2005, Mosallam and Banerjee 2007). Similarly, the experimental studies on RC T-beams, strengthened with FRP in shear have been contributed by (Chajes *et al.* 1995, Khalifa and Nanni 2000, Deniaud and Cheng 2001, 2003, Chaallal *et al.* 2002, Micelli *et al.* 2002, Bousselham and Chaallal 2006, 2008). The researchers have shown that the shear strength of reinforced concrete beams may be substantially increased by bonding fibre reinforced polymer (FRP) strips or sheets as external shear reinforcement. Most of the experimental works have been conducted by using CFRP as external shear reinforcement both for rectangular and T-beams, as compared with GFRP as external shear reinforcement. The work using GFRP as a strengthening material is very limited for RC rectangular and T-beams. Al-Sulaimani *et al.* (1994) conducted experimental studies on rectangular beams using GFRP strips and sheets as an external reinforcement and placed in the form of U-jacketing and on the sides of the beam. Cao *et al.* (2005) presented an experimental investigation on the debonding failure state of RC beams in three series with or without the use of transverse reinforcement and externally shear strengthened with complete wraps. The variables considered are shear span (a) to effective depth (d) ratio and the amount of external FRP reinforcement, but the compressive strength of concrete was same for all the series, and studied on the distribution of strains in the GFRP strips intersected by the critical shear crack and the shear capacity at debonding. Mosallam and Banerjee (2007) presented an experimental investigation on full scale RC rectangular beam specimens of three different classes unstrengthened, repaired and retrofitted and externally reinforced with FRP composites. Three composite systems namely carbon/epoxy wet layup, E-glass/epoxy wet layup and carbon/epoxy procured strips were used for retrofitted repair evaluation. Similarly, Chajes *et al.* (1995) studied the effectiveness of under-reinforced RC T-beams of small sizes for T-beams by using the externally applied composite fabrics made of aramid, E-glass, and graphite fibres, bonded to the web of the T-beam. Deniaud and Cheng (2001) conducted experimental investigation on the behaviour of full scale RC T-beams strengthened externally to the web of the T-beams. The authors studied the effect of uniaxial glass fibre, uniaxial carbon fibre, and triaxial glass fibre and the interaction of concrete, steel stirrups and external fibre-reinforced polymer sheets. Egilmez and Yormaz (2011) studied the flange and web local buckling in plastic hinge regions of steel moment frames can prevent beam column connections from achieving adequate plastic rotations under earthquake-induced forces. Experimentally investigated the effects of GFRP reinforcement on local buckling behavior of existing steel I beams with flange slenderness ratio (FSR) exceeding the slenderness limits set forth in current seismic design specifications and modified by a bottom flange triangular welded haunch. Four European HE400AA steel beams with a depth/width ratio of 1.26 and FSR of 11.4 were cyclically loaded up to 4% rotation in a cantilever beam test set-up. Both bare beams and beams

with GFRP sheets were tested in order to investigate the contribution of GFRP sheets in mitigating local flange buckling. The present paper is different from the previous investigations and focuses on the effectiveness and modes of failure of RC T-beams strengthened in shear with externally U-jacketed GFRP sheets with variation of internal transverse steel reinforcements (stirrups) and externally GFRP layers.

2. Experimental study

The parameters selected for the experimental investigation are the followings:

- (a) Three T-beam specimens without transverse steel (stirrups) and with GFRP sheet having one, two and three layers.
- (b) Three T-beam specimens with transverse steel (stirrups) spaced at 300 mm *c/c* and with GFRP sheet having one, two and three layers.
- (c) Three T-beam specimens with transverse steel (stirrups) spaced at 200 mm *c/c* and with GFRP sheet having one, two and three layers

2.1 Test specimens

The experimental program consists of eighteen (18) simply supported RC T-beams. Nine (9) beams are tested as control beam and the rest nine (9) beams are tested as strengthened beam. Nine control beams are tested in three different series. In the first series of control specimen, designated as S0, two stirrups are provided at the support and one stirrup is provided at the loading point to avoid the local shear failure. In total six numbers of stirrups are provided. In the second series of control specimens, designated as S300, the stirrups are provided at a spacing of 300 mm *c/c* whereas in the third series of specimens, designated as S200, the spacing of the stirrups is provided at 200 mm *c/c* throughout the length of the beam. The rest nine beams are strengthened for enhancing shear capacity using GFRP continuous sheet in the form of U-jacket with one, two, and three layers for each type of stirrup spacing.

The control specimens, not strengthened with GFRP, are labeled as 0L, whereas specimens strengthened with one, two, and three layer of GFRP are labeled as 1 L, 2 L, and 3 L. The series S0 refers to specimens with no transverse steel reinforcement; series S200 corresponds to specimens with steel stirrups having spacing of 200 mm and series S300 corresponds to specimens with steel stirrups having spacing of 300 mm. Thus, for example, specimen S0-0L-1 is a beam without steel stirrups (S0), without GFRP layer (0L), and sample number one whereas the strengthened specimen designated as S200-1L-CT-U-90, with steel stirrups @ 200 mm *c/c* (S200), strengthened with one layer of GFRP (1L), continuous wrapping (CT), in U-jacket around the web of the T-beams (U), and orientation of the fibre angle 90° to the longitudinal axis of the beam.

2.2 Design of specimens

All the T-beams are 2.5 m long having 250 mm flange width and 60 mm thickness, 100 mm wide web with 200 mm depth and designed to fail in shear as per Indian Standard IS 456: 2000. Based on the design, two (2) Nos. 20 mm diameter Tor steel bars are used as flexural reinforcement (area 628.31 mm²) at the bottom, and four (4) Nos. 8 mm diameter Tor steel bars are used in one layer at the top. The internal steel stirrups are 6 mm diameter and are spaced at 200 mm centres in S200 specimen and at 300 mm centres in S300 specimen respectively, whereas in S0 specimen total six number of stirrups, 2

Table 1 (a) Physical properties of cement

Characteristics	Value obtained experimentally	Test results supplied by manufacturer	Value specified by IS 8112:1989
Normal consistency, Percent	31	29	NA
Fineness (m ² /Kg)	311	308	225 (min)
Setting time, minutes			
(a) Initial	130	125	30 (min)
(b) Final	210	220	600 (max)
Specific gravity	3.10	NA	3.15
Compressive strength, MPa			
(a) 3 days	23.5	37	23 (min)
(b) 7 days	35.54	45	33 (min)
(c) 28 days	49.30	55	43 (min)

Table 1 (b) Physical properties of aggregates

Characteristics	Value obtained experimentally as per IS: 383-1970	
	Coarse aggregate	Fine aggregate
Type	Crushed	Natural
Maximum size (mm)	12.5 (Angular)	4.75
Specific gravity	2.95	2.64
Total water absorption, percent	0.53	0.30
Fineness modulus	5.00	2.73 (Grading zone II) Medium sand
Free surface moisture, percent	Nil	2

Table 2 Test results of cubes and cylinders after 28 days

Specimen designation	No. of beams	Mean cube compressive strength (MPa)	Mean cylinder Compressive strength (MPa)	Split tensile strength of cylinder (MPa)	Modulus of elasticity as per test results (MPa)
S0-0L	3	49.61	42.16	NA	3.465×10^4
S200-0L	3	59.78	42.67	NA	NA
S300-0L	3	57.62	39.53	2.70	3.624×10^4
S0-1L-CT-U-90	1				
S0-2L-CT-U-90	1	51.76	38.78	NA	3.565×10^4
S0-3L-CT-U-90	1				
S200-1L-CT-U-90	1				
S200-2L-CT-U-90	1	51.44	41.03	2.49	4.169×10^4
S200-3L-CT-U-90	1				
S300-1L-CT-U-90	1				
S300-2L-CT-U-90	1	52.06	39.35	2.74	3.657×10^4
S300-3L-CT-U-90	1				

the beam specimens of all the series. To intercept the cracks at an early stage and to improve the shear carrying capacity, the orientation of the main fibre is provided perpendicular to the longitudinal axis of the beam. The details of the specimens and experimental data on shear strengthening using GFRP are

Table 3 Mechanical properties of steel reinforcement used

Diameter (mm)	Yield stress (MPa)	Ultimate stress (MPa)	Modulus of elasticity (GPa)	Yield strain (μ strains)
20 (Tor steel)	500	590	200	2,500
8 (Tor steel)	503	646	180	2,794
6 (Mild steel)	252	461	200	

Table 4 Details of specimens and experimental data on shear strengthening using GFRP

Specimen designation	FRP config.	No. of layers	b_w mm	d mm	t_f mm	ρ_f %	ρ_s %	ρ_w %	E_f (GPa)	ε_{fu} 10^{-3}	ε_{fe} 10^{-3}
S0-0L	-	0	100	225	-	-	0	2.79	-	-	-
S300-0L	-	0	100	225	-	-	0.19	2.79	-	-	-
S200-0L	-	0	100	225	-	-	0.28	2.79	-	-	-
S0-1L-CT-U-90	CT-U	1	100	225	0.36	0.72	0	2.79	13.18	12.14	7.747
S0-2L-CT-U-90	CT-U	2	100	225	0.72	1.44	0	2.79	13.18	12.14	3.978
S0-3L-CT-U-90	CT-U	3	100	225	1.08	2.16	0	2.79	13.18	12.14	3.581
S300-1L-CT-U-90	CT-U	1	100	225	0.36	0.72	0.19	2.79	13.18	12.14	7.739
S300-2L-CT-U-90	CT-U	2	100	225	0.72	1.44	0.19	2.79	13.18	12.14	5.348
S300-3L-CT-U-90	CT-U	3	100	225	1.08	2.16	0.19	2.79	13.18	12.14	7.018
S200-1L-CT-U-90	CT-U	1	100	225	0.36	0.72	0.28	2.79	13.18	12.14	3.609
S200-2L-CT-U-90	CT-U	2	100	225	0.72	1.44	0.28	2.79	13.18	12.14	5.255
S200-3L-CT-U-90	CT-U	3	100	225	1.08	2.16	0.28	2.79	13.18	12.14	6.927

listed in Table 4.

Prior to strengthening with GFRP, the concrete surface is smoothed. A layer of epoxy based primer, which penetrates in to the concrete pores and provides better bonding to the fibres, is applied. The corners are rounded to a radius of 10 mm for avoiding the sharp edges and damage to fibre cloth. The mixing of the epoxy is done by stirring with a rod and application of epoxy on to the concrete surface is done using a brush. For first layer of GFRP, first coat of saturant resin is applied followed by the first layer of glass fibre cloth. A roller is used on the cloth surface to ensure impregnation of the fibres in the saturant and tension is maintained to minimize intrusion of air and to squeeze out the excess epoxy. The fibre cloth is then coated with a second layer of saturant resin to fully saturate the material and the excessive resin is removed by applying hard roller. The surface coating serves as a protective layer of the fibre cloth. The beams are kept for at least 7 days for epoxy to cure and harden before testing.

2.5 Test setup and Instrumentation

All specimens are tested as simple T-beams using two point loading with shear span (a) to effective depth (d) ratio equal to 3.26. The tests are carried out at the structural laboratory of Civil Engineering Department, IIT Kharagpur using 300 Ton capacity Universal Testing Machine. Fig. 2 shows the details of the test setup.

Dial gauges are used to monitor vertical displacements. One dial gauge is located at the midspan of the beam. Two are located below the loading points and the other two are located at the centre of the

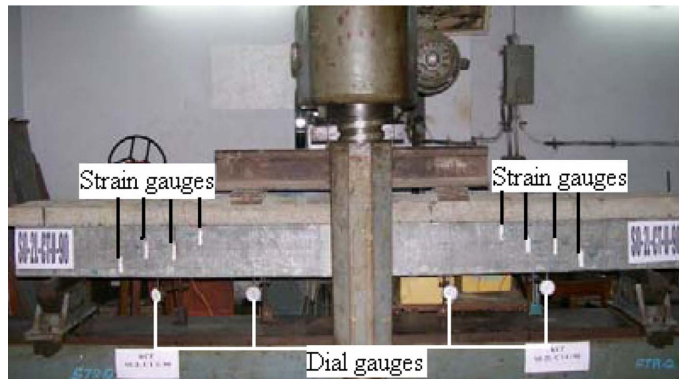


Fig. 2 Test setup

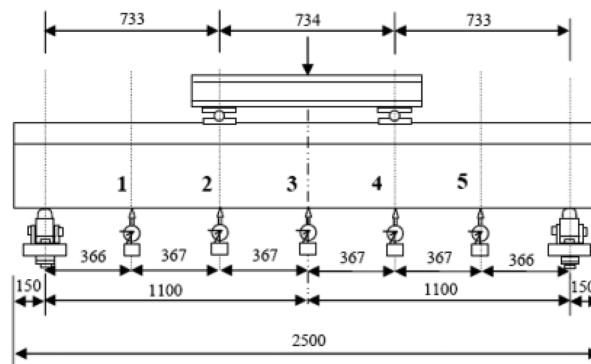


Fig. 3 Location of dial gauges

shear zone on either side as shown in Fig. 3.

Two types of electrical strain gauges namely gauges BKNIC-10 (Gauge length 10 mm, Gauge factor $2.00 \pm 2\%$, Resistance $355.0 \pm 0.5\Omega$) placed on the surface of the longitudinal and transverse steel reinforcement, and gauges BKCT-30 (Gauge length 30 mm, Gauge factor $2.00 \pm 2\%$, Resistance 350.5 ± 0.5) placed on the concrete surface are used. BKNIC-10 is attached on the longitudinal and transverse steel to measure deformation during the different stages of loading. In S0-1L-CT-U-90 and S0-2L-CT-U-90 specimens, one strain gauge (ISg1) is attached on the longitudinal steel surface at 150 mm distance from the left support, whereas in S0-3L-CT-U-90 two strain gauges (ISg1 and ISg4) are used on the longitudinal steel surface at 150 mm and 650 mm distance from the left support. In S200-1L-CT-U-90, and S200-2L-CT-U-90 three strain gauges (ISg1, ISg2 and ISg3) are attached; one in the longitudinal steel surface at 150 mm distance from the left support and the other two strain gauges are attached in stirrups in shear zone at locations (200, 90), and (400, 145) from the support. In S200-3L-CT-U-90 four strain gauges (ISg1, ISg2, ISg3 and ISg4) are attached. Similarly, in S300-1L-CT-U-90, and S300-2L-CT-U-90 specimens, three strain gauges are attached, one in the longitudinal steel surface at 150 mm distance from the left support and the other two strain gauges are attached in stirrups at locations (350, 90), and (650, 145) from the support. In S300-3L-CT-U-90 four strain gauges are attached. The details of strain gauge positions are as shown in Fig. 4.

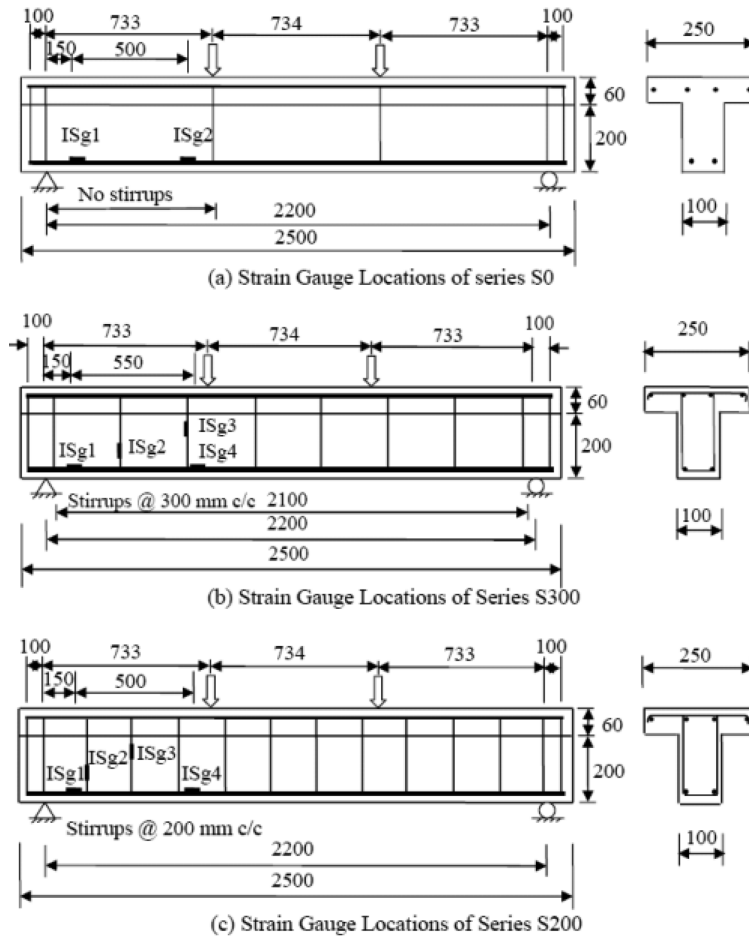


Fig. 4 Location of internal strain gauges

BKCT-30 strain gauges are attached on the concrete surface side of the web of the T-beams and to the GFRP surface on the side of the strengthened T-beams and oriented in the fibre direction. Six strain gauges are used on the concrete surface of the control beam. Three strain gauges are used at the middle of each side of the shear zone as a strain rosette. Eight strain gauges are mounted to the GFRP surface in the shear zone of the strengthened T-beams. Four strain gauges are attached on each side as per the cracking pattern of the control beam. The coordinates of strain gauges from left support considering bottom corner as (0, 0) in strengthened beam of series S0, S300, and S200 for Sg1, Sg2, Sg3, and Sg4 are (150, 50), (250, 100), (350, 100), and (450, 150) respectively. Similarly, the coordinates for Sg5, Sg6, Sg7, and Sg8 are used from right support. The details of strain gauge positions are shown in Fig. 5.

3. Analysis of test results and discussions

Table 5 shows a comparison between the experimental results of GFRP strengthened RC T-beams and shear resistance results calculated based on ACI code (ACI 440.2R-02). Different nomenclatures

Table 5 Comparison of Experimental and ACI predicted shear resistance results

Specimen designation	Experimental results						Theoretical results predicted by ACI 440.2R-02 Design approach				Modes of failure
	Load at failure (kN)	$V_{n,test}$ (kN)	$V_{c,test}$ (kN)	$V_{s,test}$ (kN)	$V_{f,test}$ (kN)	$\frac{V_{f,test}}{V_{n,test(t,uf)}} \times 100$ (%)	$V_{f,theor}$ (kN)	$V_{c,theor}$ (kN)	$V_{s,theor}$ (kN)	$\phi V_{n,theor}$ (kN)	
S0-0L	100	50	50	00	00	00	00	26.68	00	22.68	Shear failure
S300-0L	141	70.5	50	20.5	00	00	00	25.95	10.60	31.07	Shear failure
S200-0L	160	80	50	30	00	00	00	26.82	15.90	36.31	Shear failure
S0-1L-CT-U-90	136	68	50	00	18	36	6.26	25.73	00	26.25	Rupture failure
S0-2L-CT-U-90	142	71	50	00	21	42	11.84	25.73	00	30.16	GFRP debonding and rupture
S0-3L-CT-U-90	146	73	50	00	23	46	18.79	25.73	00	35.02	GFRP debonding
S300-1L-CT-U-90	156	78	50	20.5	7.5	10.64	6.26	25.90	10.60	35.54	Rupture failure
S300-2L-CT-U-90	160	80	50	20.5	9.5	13.47	12.05	25.90	10.60	39.73	GFRP debonding
S300-3L-CT-U-90	184	92	50	20.5	21.5	30.50	18.79	25.90	10.60	44.60	GFRP debonding
S200-1L-CT-U-90	182	91	50	30	11	13.75	6.26	26.37	15.90	40.45	GFRP debonding and rupture
S200-2L-CT-U-90	208	104	50	30	24	30	12.36	26.37	15.90	44.86	GFRP debonding
S200-3L-CT-U-90	192	96	50	30	16	20	18.79	26.37	15.90	49.51	GFRP debonding

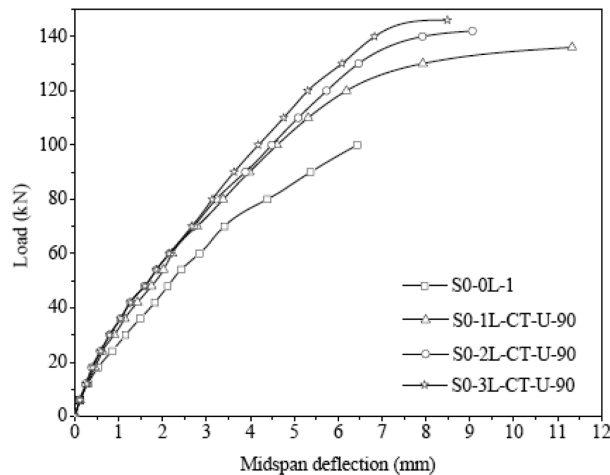


Fig. 6 Load versus midspan deflection of Series S0

applied load for the tested beams of S0, S300, and S200 series, having zero, one, two, and three layer of GFRP sheets. Fig. 9 shows the cracking pattern and modes of failure of the tested beams.

3.1 Strength

From Table 5 and Fig. 6, it may be observed that for specimen S0-1L-CT-U-90, the load at ultimate

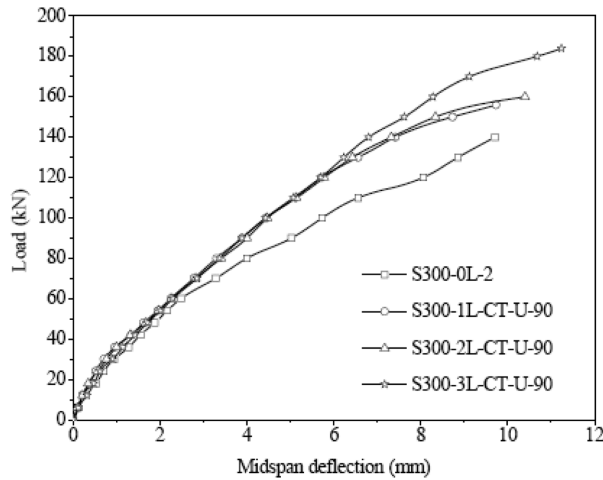


Fig. 7 Load versus midspan deflection of Series S300

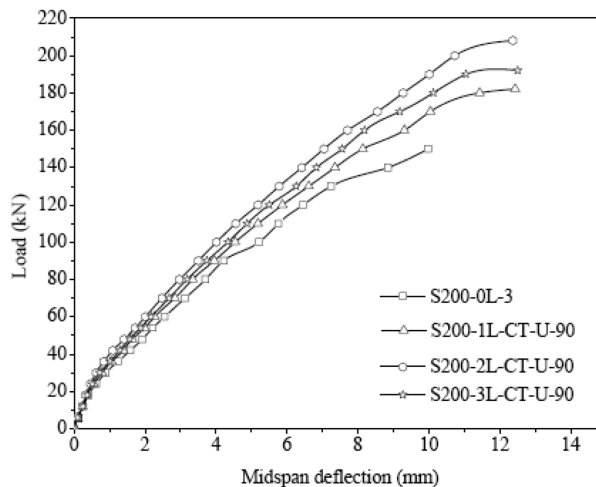
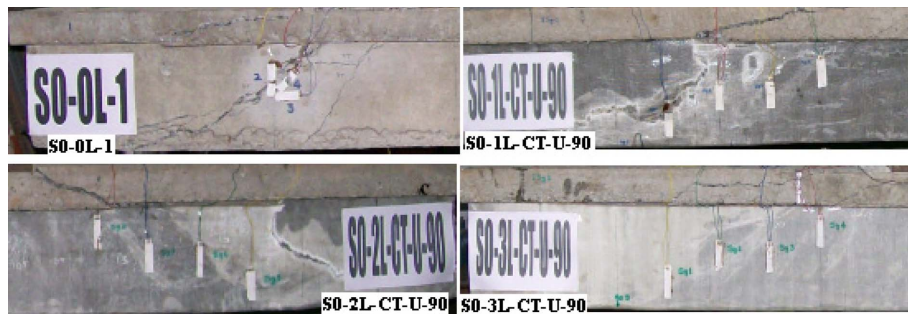


Fig. 8 Load versus midspan deflection of Series S200

failure attained 136 kN, compared to 100 kN for S0-0L specimen; that is a gain of 36%. As for the influence of the GFRP thickness on the gain in strength, the addition of second and third layer of GFRP; that is for S0-2L-CT-U-90 and S0-3L-CT-U-90 the loads at ultimate failure are 142 kN and 146 kN respectively. The percentage gain is 42% and 46% respectively as compared with control specimen S0-0L, but the gain is not appreciable, as compared with the single layer strengthened specimen.

From Table 5 and Fig. 7, it may be observed that for specimen S300-1L-CT-U-90, the load at ultimate failure attained 156 kN, compared to 141 kN for control specimen S300-0L, that is a gain of 10.64%, the addition of second and third layer of GFRP; that is for S300-2L-CT-U-90 and S300-3L-CT-U-90, the load at ultimate failure are 160 kN and 184 kN respectively. The percentage gain is 13.47% and 30.5% respectively as compared with control specimen S300-0L. It is observed that the difference in gain in shear strength of GFRP for S300-1L-CT-U-90 and S300-2L-CT-U-90 specimens is not so significant.



(a) Failure modes of tested beams-series-SO(U-Shape)



(b) Failure modes of tested beams-series-S300(U-Shape)



(a) Failure modes of tested beams-series-S200(U-Shape)

Fig. 9 Failure modes of Tested beams

Whereas in three layers S300-3L-CT-U-90 specimen, the gain in strength is more, as compared with the control specimen S300-0L.

From Table 5 and Fig. 8, it may be observed that for S200 series, the load at ultimate failure of S200-1L-CT-U-90, S200-2L-CT-U-90, and S200-3L-CT-U-90 specimens are 182 kN, 208 kN, and 192 kN respectively compared to 160 kN for control specimen S200-0L, indicating that there is a gain of 13.75%, 30%, and 20% respectively.

3.2 Deflection

As observed from Fig. 6, for S0 series, the midspan deflection in beams, strengthened with GFRP is less in comparison to the control specimen for the same amount of load. As expected, beams strengthened

with three layers of GFRP, carry more load than other specimens. However, a beam strengthened with single layer of GFRP shows more deflection than the other specimens.

Without shear reinforcement (S0 series), in S0-0L specimen, the initial cracking load is 70 kN and the deflection corresponding to this load is 3.41 mm. Ultimate failure load is 100 kN and the deflection corresponding to this load is 6.44 mm. Ductility factor in terms of deflection is 1.89. Whereas in strengthened beam, S0-1L-CT-U-90, the deflection corresponding to the cracking load is 2.8 mm. Ultimate failure load is 136 kN. The deflection corresponding to this load is 11.33 mm. Ductility factor in terms of deflection is 4.04. In strengthened beam, S0-2L-CT-U-90, deflection corresponding to the initial cracking load is 2.71 mm. Ultimate failure load is 142 kN. The deflection corresponding to this load is 9.06 mm. Ductility factor is 3.34. In strengthened beam, S0-3L-CT-U-90, deflection corresponding to the initial cracking load is 2.67 mm. Ultimate failure load is 146 kN. The deflection corresponding to this load is 8.49 mm. Ductility factor is 3.18. It is observed that the ductility factor is more in all the strengthened beams as compared with the control specimen (S0-0L). As strengthened beam is concerned, the ductility is more in single layer than two and three layers. Hence, the ductility is significant in the entire strengthened beam without shear reinforcement.

As observed from Fig. 7, for S300 series, the midspan deflection of control and strengthened beams is almost same up to 60 kN loads. Thereafter, as load increases, the deflection in beams strengthened with GFRP is less in comparison to control beams for the same amount of load. However, the deflection of the strengthened beams with different layers of GFRP is almost equal up to 120 kN load. As expected, beams strengthened with three layers of GFRP carry more load than the other two and also shows more deflection.

With shear reinforcement (S300 series), in S300-0L specimen, initial cracking load is 90 kN, the deflection corresponding to this load is 5.03 mm. Ultimate failure load is 146 kN. The deflection corresponding to this load is 9.71 mm. The ductility factor is 1.93. Whereas in strengthened beam, S300-1L-CT-U-90, the deflection corresponding to the initial cracking load is 3.89 mm. Ultimate failure load is 156 kN. The deflection corresponding to this load is 9.73 mm. The ductility factor is 2.50. In strengthened beam, S300-2L-CT-U-90, the deflection corresponding to the initial cracking load is 4.00 mm. Ultimate failure load is 160 kN. The deflection corresponding to this load is 10.4 mm. The ductility factor is 2.60. In strengthened beam, S300-3L-CT-U-90, the deflection corresponding to the initial cracking load is 3.90 mm. The ultimate failure load is 184 kN. The deflection corresponding to this load is 11.24 mm. The ductility factor is 2.90. It is observed that the ductility is more in all the strengthened beams as compared with the control specimen S300-0L. In this series, as layer increases, the ductility is also increases.

As observed from Fig. 8, the midspan deflection of control and strengthened beams of S200 series is nearly equal up to 20 kN loads. As the load increases further, the deflection in control beam specimen becomes more as compared with strengthened beams for the same load. Beam strengthened with two layers of GFRP carry more load than the others. It is also observed that all the strengthened beams of this series show almost same deflection.

With shear reinforcement (S200 series), in S200-0L specimen, initial cracking load is 90 kN, the deflection corresponding to this load is 4.22 mm. Ultimate failure load is 156 kN. The deflection corresponding to this load is 9.98 mm. The ductility factor is 2.36. Whereas in strengthened beam, S200-1L-CT-U-90, the deflection corresponding to the initial cracking load is 3.95 mm. Ultimate failure load is 182 kN. The corresponding deflection is 12.43 mm. The ductility factor is 2.89. In S200-2L-CT-U-90, the deflection corresponding to the initial cracking load is 3.50 mm. Ultimate failure load is 208 kN. The deflection corresponding to the load is 12.37 mm. The ductility factor is 3.53. In S200-

3L-CT-U-90, the deflection corresponding to the initial cracking is 3.75 mm. Ultimate failure load is 192 kN. The deflection corresponding to the failure load is 12.50 mm. The ductility factor is 3.34 mm. It is observed that the ductility is more in all the strengthened beams as compared with the control specimen S200-0L. In this series, as layer increases, the ductility is also increases up to two layers.

It may be concluded that in all the strengthened beams, the ductility is more significant in the strengthened beam without shear reinforcement and relatively less significant in the strengthened beam with shear reinforcement.

3.3 Cracking pattern and modes of failure of control and strengthened beams

The cracking pattern and failure modes of tested beams for series S0, S300, and S200 are shown in Figs. 9(a), 9(b), and 9(c). In Fig. 9(a), when control beam specimen (S0-0L-1) is loaded, it exhibited diagonal shear cracks at a load of 70 kN on both sides of the shear span. The cracks started at the centre of both the shear spans. As the load increased, the cracks widened and propagated towards the support and loading points through the flange of the T-beams, finally the failure attained at a load of 104 kN. At the time of failure, a horizontal crack appeared at the flange and it covers a distance of 275 mm approximately, thereafter, the horizontal crack inclined in approximately 15° angle for a distance of 280 mm. The shear crack angle and maximum crack width at the centre are approximately 42° and 8 mm respectively at the time of failure. In strengthened beam specimen, the rupture of GFRP layer is observed in the specimen S0-1L-CT-U-90 and S0-2L-CT-U-90. Debonding of the GFRP layer from the concrete surface is observed in the specimen S0-3L-CT-U-90 as shown in Fig. 9(a). It is observed during experimentation that at an ultimate loads of 136 kN and 142 kN, the GFRP layer gets ruptured in the specimen S0-1L-CT-U-90 and S0-2L-CT-U-90 in the same area as observed in the control beam specimen earlier. In S0-3L-CT-U-90 specimen the GFRP layer gets debonded from the concrete surface at a load of 146 kN. Also in S0-2L-CT-U-90 specimen the GFRP layer is debonded from the concrete surface immediately before the rupture failure. In these two specimens, GFRP debonding gets initiated from the top surface of the web only. At the time of ultimate failure, a horizontal crack appeared at side face of the flange for a distance of 210 mm, and then the crack got inclined for a distance of 200 mm approximately in S0-1L-CT-U-90 specimen. Some crack appears at the top of the flange and propagates in longitudinal direction for a distance of 320 mm approximately. In S0-2L-CT-U-90 specimen, the inclined crack appeared on side face of the flange and covers for a distance of 150 mm approximately, and then followed by horizontal crack for a distance of 100 mm at the flange web junction. Whereas in S0-3L-CT-U-90 specimen, the horizontal crack appeared on side face of the flange, it covers a distance of approximately 450 mm from the loading point towards support. Also two hair cracks appeared at the top of the flange from the loading point, the first one propagated along longitudinal direction, whereas the second one in transverse direction covering the full width of the flange.

In Fig. 9(b), when control beam specimen S300-0L-2 is loaded, the number of inclined shear crack appeared after 70 kN load. However, the diagonal shear crack exhibits at a load of 90 kN on both sides of shear span. The shear crack started at the centre point of the web approximately at 300 mm distance from the support. As load increased, this crack widened and propagated towards the support and loading points through the flange, finally the ultimate failure attained at a load of 146 kN. It is observed that the critical shear crack angle and maximum crack width in right shear span is 45° and 3 mm respectively. Whereas in left shear span the same are 40° and 4 mm respectively. Also a hair crack appeared at top of the flange propagated in longitudinal direction from the loading position for a distance of 185 mm and then it bends approximately in 90° angles. In strengthened beam specimen, the rupture

failure of GFRP layer in the specimen S300-1L-CT-U-90 and debonding of GFRP layer from the concrete surface of specimen S300-2L-CT-U-90 and S300-3L-CT-U-90 are observed as shown in Fig. 9b. It is observed during experimentation that at an ultimate load of 156 kN, the GFRP layer gets ruptured in the specimen S300-1L-CT-U-90 over the same shear crack location as shown in the control specimen. Whereas in S300-2L-CT-U-90 and S300-3L-CT-U-90 specimens the GFRP layer gets debonded from the concrete surface at a load of 160 kN and 184 kN respectively. Also an inclined crack appeared at the side of the flange propagates approximately 300 mm distance from the loading position. Also a crack appeared at top of the flange.

In Fig. 9(c), when beam S200-OL-3 is loaded, it exhibits diagonal shear cracks at a load of 90 kN in left side and at a load of 100 kN in right shear span of the T-beams. The crack started at the centre of both the shear spans. As load increased, this crack started to widened and propagated towards the support and loading point through the flange and leading to failure at a load of 156 kN. The maximum crack width observed at the centre in the web is 10 mm. The shear crack angle is approximately 44° in the web and almost horizontal as it reached towards the support and the flange in both shear spans. In strengthened beam specimen, the debonding of GFRP layer from the concrete surface is shown in Fig. 9(c). It is observed during experimentation that at an ultimate load of 182 kN, the GFRP layer gets debonded in the specimen S200-1L-CT-U-90. The debonding gets initiated from the top surface of the web. The GFRP layer is also observed to rupture along the diagonal shear failure line. Whereas in specimen S200-2L-CT-U-90, and S200-3L-CT-U-90 the GFRP layer gets debonded from the concrete surface at 208 kN, and 192 kN respectively. These two specimens the debonding gets initiated from the top surface of the web only, no rupture failure is observed. At the same time an inclined crack is also appeared at the side of the flange from loading points and it propagates a distance of about 185 mm, 200 mm, and 380 mm in S200-1L-CT-U-90, S200-2L-CT-U-90, and S200-3L-CT-U-90 specimens respectively.

4. Comparison of Test Results with ACI predictions

The shear resistance due to GFRP obtained by tests is compared to the nominal shear resistance predicted by the ACI 440.2R-02 guidelines are listed in Table 5. It may be observed that the $V_{f,test}$ result gives higher value than the $V_{f,theor}$ results in all the specimens of series S0. However, as number of layer increases the difference between the test and theoretical results approach towards closer value. Whereas in series S300 for one and three layers $V_{f,test}$ results give slightly higher value than the $V_{f,theor}$ results, and for two layers $V_{f,theor}$ result gives slightly more than $V_{f,test}$ results, but in series S200, $V_{f,test}$ results give higher value up to two layers than the $V_{f,theor}$ results, thereafter, as layer increases, gives slightly lower value.

It may be concluded that the ACI design approaches give conservative results for T-beams strengthened in shear with externally U-jacketed GFRP sheets of the entire specimen in series S0, whereas in S300 series the design approach gives almost equal values and in S200 series up to two layers gives conservative value. It indicates that, the strengthened beam without transverse steel reinforcement and with single layer of GFRP sheet, the ACI design approach gives more conservative result. As layer increases the ACI design approach gives less conservative. The strengthened beam with transverse steel reinforcement in S300 series for one and three layer of GFRP, the ACI design approach gives relatively less conservative, whereas with two layers the ACI result shows slightly higher value than the test value. In S200 series, the ACI result gives a conservative value up to two layers, and in three layers specimen, the predicted value is slightly higher than the test value.

5. Summary and conclusions

This study presents the results of an experimental investigation involving eighteen full scale simply supported RC T-beams strengthened in shear with externally bonded GFRP sheets, in three series, with and without the transverse steel reinforcement. The test results clearly indicate that for RC T-beams strengthened in shear with U-jacketed GFRP sheet, increase the effectiveness by 10~46%.

The important observations that emerge from this study are as follows:

1. The gain in shear capacity is significant in all the GFRP strengthened RC T-beams. But so far as the number of layers is concerned, one layer is more effective than two and three layers.
2. The modes of failure of strengthened RC T-beams in shear with U-jacketed GFRP wrap clearly indicates that, in single layer jacketing, the failure is due to GFRP rupture, where as for two and three layers, the failure is due to GFRP debonding.
3. The addition of internal transverse steel resulted in a significant decrease of the gain in shear capacity due to GFRP. But the combination of layer and transverse steel is an important factor to gain the shear capacity. The combination of three layers with internal transverse steel in S300 series resulted good effectiveness as compared with one and two layers. But in S200 series, up to two layers resulted better effectiveness.
4. The load-deflection graph clearly indicates that the RC T-beams strengthened in shear with GFRP sheets have a significant effect on beams ductility. The RC T-beams, becomes more flexible and more deformable, after strengthened by GFRP sheets.

Acknowledgments

The authors would like to thank the Indian Institute of Technology, Kharagpur for the financial support, and material support to their research work. The authors also express their sincere gratitude to all staff members of the structural engineering laboratory, IIT Kharagpur, India, for their technical support throughout the experimental work.

References

- American Concrete Institute (ACI). (2002), "Building code requirements for reinforced concrete (ACI 318-02) and commentary", *318RM-02*, Detroit.
- ACI 440.2R-02. (2002), "Guide for the design and construction of externally bonded FRP systems for strengthening concrete structures", *ACI Committee 440*, Farmington Hills, Michigan, 45 p.
- Al-Sulaimani, G.J., Sharif, A., Basunbul, I.A., Baluch, M.H. and Ghaleb, B.N. (1994), "Shear repair for reinforced concrete by fiberglass plate bonding", *ACI Struct. J.*, **91**(3), 458-464.
- Adhikary, B.B., Mutsuyoshi, H. and Ashrof, M. (2004), "Shear strengthening of reinforced concrete beams using fiber reinforced polymer sheets with bonded anchorage", *ACI Struct. J.*, **101**(5), 660-668.
- Berset, J.D. (1992), "Strengthening of reinforced concrete beams for shear using FRP composites", *MS thesis*, Dept. of Civil and Environmental engineering, MIT.
- Bousselham, A. and Chaallal, O. (2004), "Shear strengthening reinforced concrete beams with fiber-reinforced polymer: assessment of influencing parameters and required research", *ACI Struct. J.*, **101**(2), 219-227.
- Bousselham, A. and Chaallal, O. (2006), "Effect of transverse steel and shear span of the performance of RC beams strengthened in shear with CFRP", *Composites: Part B*, **37**(1), 37-46.
- Bousselham, A. and Chaallal, O. (2008), "Mechanisms of shear resistance of concrete beams strengthened in

- shear with externally bonded FRP”, *J. Compos. Constr.*, **12**(5), 499-512.
- Cao, S.Y., Chen, J.F., Teng, J.G., Hao, Z. and Chen, J. (2005), “Debonding in RC beams shear strengthened with complete FRP wraps”, *J. Compos. Constr.*, **9**(5), 417-428.
- Chaallal, O., Nollet, M.J. and Perraton, D. (1998), “Shear strengthening of RC beams by externally bonded side CFRP strips”, *J. Compos. Constr.*, **2**(2), 111-113.
- Chaallal, O., Shahawy, M., and Hassan, M. (2002), “Performance of reinforced concrete T-Girders strengthened in shear with carbon fiber-reinforced polymer fabric”, *ACI Struct. J.*, **99**(3), 335-343.
- Chajes, M.J., Januszka, T.F., Mertz, D.R., Thomson, T.A., Jr. and Finch, W.W., Jr. (1995), “Shear strengthening of reinforced concrete beams using externally applied composite fabrics”, *ACI Struct. J.*, **92**(3), 295-303.
- Chen, J.F. and Teng, J.G. (2003a), “Shear capacity of FRP-strengthened RC beams: FRP debonding”, *Constr. Build. Mater.*, **17**(1), 27-41.
- Chen, J.F. and Teng, J.G. (2003b), “Shear capacity of fiber-reinforced polymer strengthened RC beams: Fiber reinforced polymer rupture”, *J. Struct. Engrg.*, **129**(5), 615-625.
- Deniaud, C. and Cheng, J.J.R. (2001), “Shear behavior of reinforced concrete T-beams with externally bonded fiber-reinforced polymer sheets”, *ACI Struct. J.*, **98**(3), 386-394.
- Deniaud, C. and Cheng, J.J.R. (2003), “Reinforced concrete T-beams strengthened in shear with fiber reinforced polymer sheets”, *J. Compos. Constr.*, **7**(4), 302-310.
- Egilmez, O. O. and Yormaz, D. (2011), “Cyclic testing of steel I-beams reinforced with GFRP”, *Steel and Compos. Struct. An International Journal*, **11**(2).
- Indian Standard (IS). (2000), “Plain and reinforce concrete code of practice IS 456:2000”, India, 100p.
- Khalifa, A., Gold, W.J., Nanni, A. and Aziz, A. (1998), “Contribution of externally bonded FRP to shear capacity of RC flexural members”, *J. Compos. Constr.*, **2**(4), 195-201.
- Khalifa, A. and Nanni, A. (2000), “Improving shear capacity of existing RC T-section beams using CFRP composites”, *Cement and Concrete Composites*, **22**(3), 165-174.
- Khalifa, A. and Nanni, A. (2002), “Rehabilitation of rectangular simply supported RC beams with shear deficiencies using CFRP composites”, *Construction and Building Materials*, **16**(3), 135-146.
- Li, A., Assih, J., and Delmas, Y. (2001), “Shear strengthening of RC beams with externally bonded CFRP sheets”, *J. Struct. Engrg.*, **127**(4), 374-380.
- Li, A., Diagona, C. and Delmas, Y. (2002), “Shear strengthening effect by bonded composite fabrics on RC beams”, *Composites: Part B*, **33**(3), 225-239.
- Malek, A.M. and Saadatmanesh, H. (1998), “Ultimate shear capacity of reinforced concrete beams strengthened with web-bonded Fiber-reinforced plastic plates”, *ACI Struct. J.*, **95**(4), 391-399.
- Micelli, F., Anniah, R.H. and Nanni, A. (2002), “Strengthening of short shear span reinforced concrete T joists with fiber reinforced plastic composites”, *J. Compos. Constr.*, **6**(4), 264-271.
- Mosallam, A.S. and Banerjee, S. (2007), “Shear enhancement of reinforced concrete beams strengthened with FRP composite laminates”, *Composites: Part B*, **38**(5-6), 781-793.
- Noris, T., Saadatmanesh, H. and Ehsani, M.R. (1997), “Shear and flexural strengthening of RC beams with carbon fiber sheets”, *J. Struct. Engrg.*, **123**(7), 903-911.
- Pellegrino, C. and Modena, C. (2002), “Fiber reinforced polymer shear strengthening of reinforced concrete beams with transverse steel reinforcement”, *J. Compos. Constr.*, **6**(2), 104-111.
- Taljsten, B., Elfgren, L. (2000), “Strengthening concrete beams for shear using CFRP-materials: evaluation of different application methods”, *Composites Part B: Engineering*, **31**(2), 87-96.
- Taljsten, B. (2003), “Strengthening concrete beams for shear with CFRP sheets”, *Constr. Build. Mater.*, **17**(1), 15-26.
- Triantafillou, T.C. (1998), “Shear strengthening of reinforced concrete beams using epoxy bonded FRP composites”, *ACI Struct. J.*, **95**(2), 107-115.
- Triantafillou, T.C. and Antonopolous, C.P. (2000), “Design of concrete flexural members strengthened in shear with FRP”, *J. Compos. Constr.*, **4**(4), 198-205.
- Zhang, Z., and Hsu, C.T.T. (2005), “Shear strengthening of reinforced concrete beams using carbon-fiber-reinforced polymer laminates”, *J. Compos. Constr.*, **9**(2), 158-169.

Notation

The following symbols are used in this paper:

a	=	shear span, mm
A_c	=	area of concrete cross section, mm ²
A_f	=	area of GFRP external shear reinforcement = $2t_f w_f$, mm ²
A_{sl}	=	total area of longitudinal steel reinforcement, mm ²
A_{sw}	=	total area of transverse steel reinforcement, mm ²
b_w	=	width of the beam cross-section, mm
d	=	depth from the top of the section to the centre of tension steel reinforcement, mm
d_f	=	effective depth of the GFRP shear reinforcement, mm
E_f	=	elastic modulus of GFRP, GPa
E_s	=	elastic modulus of steel reinforcement, GPa
s_f	=	spacing of GFRP strips, mm
t_f	=	thickness of GFRP sheet on one side of the beam, mm
$V_{c,test}$	=	nominal shear strength provided by concrete (experimental value)
$V_{c,theor}$	=	nominal shear strength provided by concrete (theoretical value)
$V_{f,test}$	=	nominal shear strength provided by GFRP shear reinforcement (experimental value)
$V_{f,theor}$	=	nominal shear strength provided by GFRP shear reinforcement (theoretical value)
$V_{n,test}$	=	nominal shear strength (experimental value)
$V_{n,theor}$	=	nominal shear strength (theoretical value)
$V_{s,test}$	=	nominal shear strength provided by steel shear reinforcement (experimental value)
$V_{s,theor}$	=	nominal shear strength provided by steel shear reinforcement (theoretical value)
w_f	=	width of GFRP strips, mm
ε_{fe}	=	effective strain in GFRP sheet
ε_{fu}	=	ultimate tensile strain of fibre material in the GFRP composite
ϕ	=	strength reduction factor
ρ_f	=	GFRP shear reinforcement ratio = $(2t_f / b_w)(w_f / s_f)$
ρ_s	=	transverse steel reinforcement ratio = $A_{sw} / (sb_w)$
ρ_w	=	Longitudinal steel reinforcement ratio = $A_{sl} / (b_w d)$